A review of studies on fluid flow passing through an ideal aggregate Part I: Models with an uniformly permeable porous layer

Rong Yuan
Qingdao University
College of Mathematics
308 Ningxia Road, Qingdao, Shandong 266071
P. R. China
yrong111@yahoo.com

Abstract: This is a review of studies on fluid flow passing through an isolated ideal aggregate with a porous layer with the uniformly permeability. Fluid flows are governed by the Brinkman's extension of Darcy's law and continuity equation. These equations with appropriate boundary conditions are analytically solved by introducing stream functions, respectively. The comparisons between Kim & Yuan's cell model with a porous layer with the uniformly permeability and other previous works are investigated.

Key–Words: ideal aggregate; porous media; uniformly permeability; drag force

1 Introduction

Fluids are substances whose molecular structure offers no resistance to external shear forces: even the smallest force causes deformation of fluid particles. Fluid flow is caused by the action of externally applied forces. Common driving forces include pressure differences, gravity, shear, rotation, and surface tension. The effect of the driving forces differ considerably when fluids pass objects with different permeabilities so that fluid behavior changes significantly. Therefore, study of the hydrodynamics of fluid flow passing impermeable or porous objects is important in the theory of fluid dynamics.

Porous media can be found in many instances in natural and engineered systems such as soil and rocks in nature; animal and plant tissues in biology [10, 17]; and aggregates formed during sedimentation and granular filtration in water and wastewater treatment. When fluid flows pass through these porous medium, the characteristics of flows are closely related to the hydrodynamic properties of the porous medium. For example, in water and wastewater treatment using membrane filtration, the product flow and membrane life-span are affected by hydrodynamic properties of the porous medium such as permeability and selectivity. Therefore, study for hydrodynamics of fluid flow passing through porous media is very important in real applications.

Fluid flow relative to aggregates of fine particles is also of significance in processes of conventional water and wastewater treatment such as coagulation/flocculation, sedimentation, and granular filtration as well as advanced treatment such as membrane filtration [1, 13, 22, 25, 26, 28, 31, 41, 43, 44].

There are four pressure-driven membrane separation process: Microfiltration (MF), Ultrafiltration (UF), Nanofiltration (NF) and Reverse Osmosis (RO). MF removes contaminants from a fluid by passage through a microporous membrane. A typical microfiltration membrane pore size range is 0.1 to $10\mu m$. UF is a variety of membrane filtration in which hydrostatic pressure forces a liquid against a semipermeable membrane. Suspended solids and solutes of high molecular weight are retained, while water and low molecular weight solutes pass through the membrane. This separation process is used in industry and research for purifying and concentrating macromolecular (10^3 - 10^6 Da) solutions, especially protein solutions. NF is a relatively recent membrane process used most often with low total dissolved solids water such as surface water and fresh groundwater to soften water (polyvalent cation removal) and remove disinfection by-product precursors such as natural organic matter and synthetic organic matter. NF is widely used in food processing applications such as dairy for simultaneous concentration and partial (monovalent ion) demineralization. RO is a separation process that uses pressure to force a solution through a membrane that retains the solute on one side and allows the pure solvent to pass to the other side. More formally, it is the process of forcing a solvent from a region of high solute concentration through a membrane to a region of low solute concentration by applying a pressure in excess of the osmotic pressure. This is the reverse

of the normal osmosis process, which is the natural movement of solvent from an area of low solute concentration, through a membrane, to an area of high solute concentration when no external pressure is applied. The membrane here is semipermeable, meaning it allows the passage of solvent but not of solute.

MF and UF are widely used for particulate removal, capable of separating particulate materials ranging from 10 nm to 10 microns. In the processes of MF/UF, particles within the feed stream are subjected to a drag force and accumulate near the membrane surface and tend to axially migrate to the outlet of the membrane. The boundary layer concentration modifies the solution properties of viscosity and density, and solute molecular diffusivity [29]. During MF and UF processes, flux decline occurs due to various fouling phenomena such as concentration polarization, deposition and adsorption of retained solutes on membrane surfaces, and pore blocking/plugging of membranes.These phenomena result in a decreasing driving force on permeation due to enhanced resistances against solvent transport through membranes [4, 5, 11, 12, 38, 39]. In MF and UF processes, aggregate cake formation is one pattern of matter-stacking phenomena on the membrane surfaces, while other patterns cause distinguishable behaviors of permeate flux decline [2, 3, 6, 8, 9, 18, 24, 32, 33, 34, 35, 36, 37, 47, 48].

The major limiting factor of filtration performance is the ratio of permeate flux (with appropriate water quality) to operation/maintenance cost, often increasing due to membrane fouling. When coagulation/flocculation of the conventional water and wastewater treatment is used as a pretreatment or coprocess of MF/UF applications, a higher permeate flux is observed because deposited aggregates generate much more porous and permeable structures than those of cake layers composed of individual colloidal particles. This phenomenon, so-called aggregate-enhanced membrane filtration (AEMF),[14, 19, 20, 23, 28, 31, 42, 45, 46], has significant potential in optimizing MF/UF processes and possibly minimizing the operation/maintenance cost, but it has not been fully addressed with rigorous fundamentality. An in-depth analysis of fluid flow relative to the aggregates will, therefore, lead to a better understanding of AEMF.

2 Drag force exerted on isolated spherical objects

The study for hydrodynamics of fluid flow relative to an impermeable sphere dates back to about 150 years ago [40]. Fluid flow was governed by the Stokes equation and continuity equation. Almost 100 years later, Brinkman [7] studied fluid flow passing through an isolated sphere of uniform permeability. In 1987 [27], Masliyah, et al. combined Stokes' and Brinkman's models together and studied the creeping flow past a solid sphere with a uniformly porous shell.

2.1 Stokes' model

In 1851 [40], Stokes studied the effect of the internal friction of fluids on the motion of pendulums. As one of the applications of the theory, he investigated the hydraulic resistance of a sphere moving uniformly in a homogeneous fluid, which can be obtained as a limiting case of the resistance to a ball pendulum.

Let $\mathbf{u}$ be the fluid velocity and u_r,u_θ and u_ϕ the components of the velocity along the spherical coordinate system of r, θ and ϕ, respectively, p the pressure, and μ the viscosity of the fluid. When the fluid is homogeneous, incompressible, and Newtonian, the governing equations are

$$\mu\nabla^2\mathbf{u} = \nabla p \tag{1}$$

and continuity equation

$$\nabla\cdot\mathbf{u} = 0 \tag{2}$$

Besides the general equations of Eqs.(1) and (2), boundary equations of the fluid flow need to be considered. For convenience, there will be no occasion to consider the case of a free surface, only that of the common surface of the fluid and a solid. If the fluid immediately in contact with a solid could flow past it with a finite velocity, it would follow that the solid was infinitely smoother with respect to its action on the fluid than the fluid with respect to its action on itself. Let R be the radius of the solid whose center is located at the origin of spherical coordinates (r, θ, ϕ). The fluid flow approaches in the $+Z$ direction with velocity V, as depicted in Figure 1, due to the axisymmetry of the fluid flow relative to an isolated permeable sphere. The boundary conditions are as follows:

$$u_r(R,\theta) = 0 \tag{3a}$$
$$u_\theta(R,\theta) = 0 \tag{3b}$$
$$\lim_{r\to+\infty} u_r(r,\theta) = V\cos\theta \tag{3c}$$
$$\lim_{r\to+\infty} u_\theta(r,\theta) = -V\sin\theta \tag{3d}$$

To solve the governing equations of Eqs. (1) and (2) with boundary conditions (3), Stokes introduced a stream function $\psi(r,\theta)$ which satisfies the following

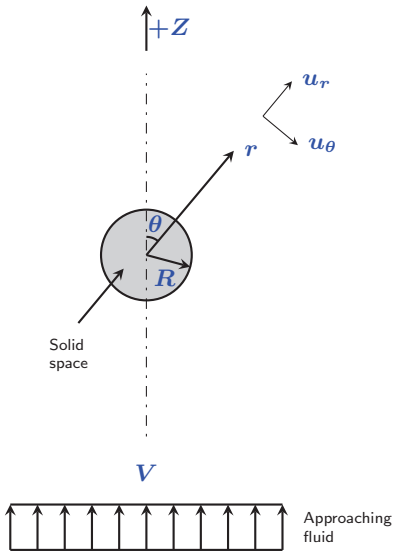

Figure 1: Coordinate system for axi-symmetric fluid flow relative to a solid sphere

equations:

$$u_r = -\frac{1}{r\sin^2\theta}\frac{\partial\psi}{\partial\theta} \tag{4a}$$

$$u_\theta = \frac{1}{r\sin\theta}\frac{\partial\psi}{\partial r} \tag{4b}$$

Then the governing equations (1) and (2) become the following partial differential equations in a form of the stream function $\psi(r,\theta)$:

$$E^4\psi = 0 \tag{5}$$

where E^2 is a differential operator defined as

$$E^2 = \frac{\partial^2}{\partial r^2} + \frac{\sin\theta}{r^2}\frac{\partial}{\partial\theta}\left(\frac{1}{\sin\theta}\frac{\partial}{\partial\theta}\right) \tag{6}$$

The general solution of Eq. (5) is:

$$\psi = \frac{1}{2}V\left(\frac{A}{r} + Br + Cr^2 + Dr^4\right)\sin^2\theta \tag{7}$$

where coefficients A, B, C and D are determined by using the boundary conditions (3) as follows:

$$A = \frac{R^3}{2},\ B = -\frac{3R}{2},\ C = 1,\ \text{and}\ D = 0 \tag{8}$$

Stokes [40] also calculated the drag force exerted on the solid sphere

$$\mathbf{F} = 2\pi R^2\int_0^\pi (-\tau_{rr}\cos\theta + \tau_{r\theta}\sin\theta)|_{r=R}\sin\theta d\theta \tag{9}$$

where τ_{rr} and $\tau_{r\theta}$ are normal and tangential components of the stress tensors of fluid flow, respectively. They are defined as follows:

$$\tau_{rr} = -p + 2\mu\frac{\partial u_r}{\partial r} \tag{10a}$$

$$\tau_{r\theta} = \mu\left(\frac{1}{r}\frac{\partial u_r}{\partial\theta} + \frac{\partial u_\theta}{\partial r} - \frac{u_\theta}{r}\right) \tag{10b}$$

Using Stokes' law, the dimensionless drag force Ω is introduced as

$$\Omega = \frac{\mathbf{F}}{6\pi\mu V R^2} \tag{11}$$

then, it is represented as

$$\Omega = -\frac{2B}{3R} \tag{12}$$

components of the flow velocity are

$$u_r = \left(1 + \frac{1}{2}\frac{R^3}{r^3} - \frac{3}{2}\frac{R}{r}\right)\cos\theta V \tag{13}$$

and

$$u_\theta = \left(-1 + \frac{1}{4}\frac{R^3}{r^3} + \frac{3}{4}\frac{R}{r}\right)\sin\theta V \tag{14}$$

and, therefore the dimensionless drag force is

$$\Omega_S = 1 \tag{15}$$

2.2 Brinkman's model

Brinkman [7] studied a solution of long chain molecules in which each polymer molecule forms a molecular cluster. He also studied sedimentation velocity of the molecular cluster and the viscosity of such solutions. According to this model, each molecular cluster is represented by a porous sphere which has a constant hydraulic permeability. Similar to Stokes's model, let R be the radius of the porous sphere which centers at the origin of spherical coordinates (r, θ, ϕ), and the flow approaches to the sphere in the $+Z$ direction with a uniform velocity V, as shown in Figure 2 Let $\mathbf{u}$ be the fluid velocity outside the porous sphere, $\mathbf{u}^* = (u_r^*, u_\theta^*, u_\phi^*)$ the velocity of fluid through the porous sphere. The azimuthal component of $\mathbf{u}^*$, u_ϕ^*, is zero due to the spherical symmetry. According to Brinkman, the fluid flow through the porous sphere is governed by the extension of Darcy's law (so called Brinkman's extension of Darcy's law or Brinkman's Equation [7]. The governing equations outside and inside of the porous sphere are

$$\mu\nabla^2\mathbf{u} = \nabla p, \quad r > R \tag{16a}$$

$$\mu^*\nabla^2\mathbf{u}^* - \frac{\mu^*}{\kappa}\mathbf{u}^* = \nabla p^*, \quad 0 < r < R \tag{16b}$$

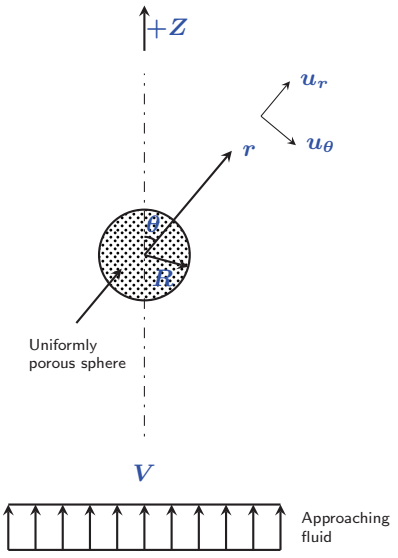

Figure 2: Coordinate system for axi-symmetric fluid flow relative to a porous sphere

respectively, and the continuity equations are,

$$\nabla \cdot \mathbf{u} = 0, \quad r > R \tag{17a}$$
$$\nabla \cdot \mathbf{u}^* = 0, \quad 0 < r < R \tag{17b}$$

where p and p^* are pressures, μ and μ^* viscosities of fluid, and κ is the permeability of the uniformly porous sphere.

It is assumed that the velocity of fluid flow at the center of the porous sphere is finite, the normal and tangential components of velocity and stress tensor across the porous sphere interface are continuous, and the flow is unidirectional far from the permeable sphere. So the boundary conditions are

$$\lim_{r\to 0} u_r^* \text{ is finite} \tag{18a}$$
$$\lim_{r\to 0} u_\theta^* \text{ is finite} \tag{18b}$$
$$u_r(R,\theta) = u_r^*(R,\theta) \tag{18c}$$
$$u_\theta(R,\theta) = u_\theta^*(R,\theta) \tag{18d}$$
$$\tau_{rr}(R,\theta) = \tau_{rr}^*(R,\theta) \tag{18e}$$
$$\tau_{r\theta}(R,\theta) = \tau_{r\theta}^*(R,\theta) \tag{18f}$$
$$\lim_{r\to\infty} u_r = V\cos\theta \tag{18g}$$
$$\lim_{r\to\infty} u_\theta = -V\sin\theta \tag{18h}$$

where ${\tau_{rr}}^*$ and ${\tau_{r\theta}}^*$ are normal and tangential components of the stress tensors inside the porous sphere, respectively, which are defined as follows:

$$\tau_{rr}^* = -p^* + 2\mu^* \frac{\partial u_r^*}{\partial r} \tag{19a}$$
$$\tau_{r\theta}^* = \mu^* \left(\frac{1}{r}\frac{\partial u_r^*}{\partial \theta} + \frac{\partial u_\theta^*}{\partial r} - \frac{u_\theta^*}{r} \right) \tag{19b}$$

With the incompressibility of the Newtonian fluid implied in Eq. (17), it has been proven that the continuity of the normal stress is equivalent to that of the fluid pressure [14, 23]:

$$p^*(R,\theta) = p(R,\theta) \tag{20}$$

Similar to Eq. (4), $\psi^*(r,\theta)$ is defined

$$u_r^* = -\frac{1}{r^2\sin\theta}\frac{\partial \psi^*}{\partial \theta} \tag{21a}$$
$$u_\theta^* = \frac{1}{r\sin\theta}\frac{\partial \psi^*}{\partial r} \tag{21b}$$

Then, the governing Eqs.(16) and (17) are combined into the 4th order partial differential equations

$$E^4\psi = 0, \quad r > R \tag{22a}$$
$$E^4\psi^* - \frac{1}{\kappa}E^2\psi^* = 0, \quad 0 < r < R \tag{22b}$$

where E^2 is defined by the Eq. (6). The general solutions of Eq. (22) are

$$\psi = -\frac{\kappa V}{2}\left(\frac{A}{\xi} + B\xi + C\xi^2 + D\xi^4\right)\sin^2(\theta), \quad \xi > \beta \tag{23a}$$
$$\psi^* = -\frac{\kappa V}{2}\left[\frac{E}{\xi} + F\xi^2 + G\left(\frac{\cosh\xi}{\xi} - \sin\xi\right) + H\left(\frac{\sinh\xi}{\xi} - \cosh\xi\right)\right]\sin^2(\theta), \quad 0 < \xi < \beta \tag{23b}$$

where $\xi = r/\sqrt{\kappa}$ and $\beta = R/\sqrt{\kappa}$. Using boundary conditions of Eq. (18), one can determine coefficients $A - H$ as follows:

$$A = \frac{\beta^3}{J_B}\left[-2\beta^2 + 3\left(\beta^2+2\right)\left(1 - \frac{\tanh\beta}{\beta}\right)\right] \tag{24a}$$
$$B = -\frac{3\beta^3}{J_B}\left(1 - \frac{\tanh\beta}{\beta}\right) \tag{24b}$$
$$C = 1 \tag{24c}$$
$$D = 0 \tag{24d}$$
$$E = 0 \tag{24e}$$
$$F = \frac{3}{J_B}\left(1 - \frac{\tanh\beta}{\beta}\right) \tag{24f}$$
$$G = 0 \tag{24g}$$
$$H = \frac{6\beta^2}{J_B}\cdot\frac{1}{\cosh\beta} \tag{24h}$$

where $J_B = 2\beta^2 + 3\left(1 - \dfrac{\tanh\beta}{\beta}\right)$. The dimensionless drag force Ω_B is:

$$\Omega_B = -\frac{2B}{3\beta} = \frac{2\beta^2\left(1 - \dfrac{\tanh\beta}{\beta}\right)}{2\beta^2 + 3\left(1 - \dfrac{\tanh\beta}{\beta}\right)} \tag{25}$$

For a impermeable solid sphere, $\kappa \to 0$, i.e., $\beta \to \infty$ and $\tanh\beta/\beta \to 0$. In this case, Ω_B of Eq. (15) converges to $\Omega_S(=1)$.

2.3 Masliya et al.'s model

Masliya et al [27] studied creeping flow past a solid sphere with a porous shell by combining the Stokes and Brinkman models. The dimensionless radius of solid core and shell thickness, normalized by the square root of the shell permeability, govern the fluid flow inside and outside the porous shell. In the limiting cases, the analytical solution describing the flow past the composite sphere reduces to those for flow past a solid sphere (Stokes' case [40]) and a homogeneous porous sphere (Brinkman's case [7]).

Let b be the outer radius of the porous shell of the isolated composite sphere and a the radius of the solid impermeable sphere surrounded by the porous shell. It is assumed that the porous shell is homogeneous and isotropic with a constant permeability κ. The creeping flow of the Newtonian fluid of viscosity μ is assumed to be steady and axi-symmetric. For convenience, the authors considered the sphere to be stationary having its center at the origin of spherical coordinates (r, θ, ϕ), while a constant fluid is approaching in the $+Z$ direction at velocity V, as shown in Figure 3. Let $\mathbf{u} = (u_r, u_\theta, u_\phi)$ and $\mathbf{u}^* = ({u_r}^*, {u_\theta}^*, {u_\phi}^*)$ denote the velocity vectors of fluid flow through the outside of the composite sphere and the porous shell, respectively. The governing equations are as follows:

$$\mu\nabla^2\mathbf{u} = \nabla p, \quad r > b \tag{26a}$$

$$\mu^*\nabla^2\mathbf{u}^* - \frac{\mu^*}{\kappa}\mathbf{u}^* = \nabla p^*, \quad a < r < b \tag{26b}$$

the continuity equations of

$$\nabla\cdot\mathbf{u} = 0, \quad r > b \tag{27a}$$

$$\nabla\cdot\mathbf{u}^* = 0, \quad a < r < b \tag{27b}$$

where μ, μ^*, p, p^* and κ have the same meanings as described above. The pressure profiles of p and p^* satisfy the following equation:

$$p(b,\theta) = p^*(b,\theta) \tag{28}$$

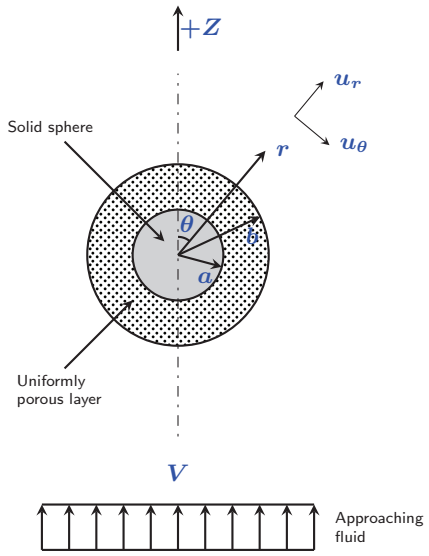

Figure 3: Coordinate system for axi-symmetric fluid flow relative to a composite sphere comprising a solid impermeable sphere surrounded by a uniformly porous shell

and

$$\mu = \mu^* \tag{29}$$

is assumed [14, 24].

For the present problem, the boundary conditions are described as follows:

$$u_r^*(a,\theta) = 0 \tag{30a}$$

$$u_\theta^*(a,\theta) = 0 \tag{30b}$$

$$u_r(b,\theta) = u_r^*(b,\theta) \tag{30c}$$

$$u_\theta(b,\theta) = u_\theta^*(b,\theta) \tag{30d}$$

$$\tau_{rr}(b,\theta) = \tau_{rr}^*(b,\theta) \tag{30e}$$

$$\tau_{r\theta}(b,\theta) = \tau_{r\theta}^*(b,\theta) \tag{30f}$$

$$\lim_{r\to\infty} u_r = V\cos\theta \tag{30g}$$

$$\lim_{r\to\infty} u_\theta = -V\sin\theta \tag{30h}$$

In the limit of $a = b = R$, Eq. (30) is identical to Eq. (18)

To solve the governing equation (26) and (27) with the boundary conditions of Eq. (30), the stream functions ψ and ψ^* of Eq. (23) satisfy the following partial differential equations:

$$E^4\psi = 0, \quad r > b \tag{31a}$$

$$E^4\psi^* - \frac{1}{\kappa}E^2\psi^* = 0, \quad a < r < b \tag{31b}$$

The general solutions of the stream functions $\psi(\xi,\theta)$ and $\psi^*(\xi,\theta)$ can be expressed as follows, which are

similar to Eq. (7) and Eq. (23), respectively.

$$\psi = -\frac{\kappa V}{2}\left(\frac{A}{\xi}+B\xi+C\xi^2+D\xi^4\right)\sin^2(\theta), \quad \xi>\beta \tag{32a}$$

$$\psi^* = -\frac{\kappa V}{2}\left[\frac{E}{\xi}+F\xi^2+G\left(\frac{\cosh\xi}{\xi}-\sin\xi\right) +H\left(\frac{\sinh\xi}{\xi}-\cosh\xi\right)\right]\sin^2(\theta), \quad \alpha<\xi<\beta \tag{32b}$$

where $\xi = r/\sqrt{\kappa}$, $\alpha = a/\sqrt{\kappa}$ and $\beta = b/\sqrt{\kappa}$. In terms of functional forms, Eqs. (7) and (32a) are identical using r and ξ, respectively; Eqs. (23b) and (32b), of the same form, are applied to different radical ranges.

Using the boundary conditions of Eq. (30), these coefficients from A to H are determined as follows:

$$B = \frac{1}{2J_M}\left[\left(3\,\alpha^3-9\,\beta\,\alpha^2+9\,\alpha+6\,\beta^3\right)\sinh\Delta +\left(-3\,\beta\,\alpha^3+9\,\alpha^2-9\,\beta\,\alpha-6\,\beta^4\right)\cosh\Delta\right] \tag{33}$$

where

$$J_M = \left(3\,\alpha^2-3\right)\sinh\Delta +\left(\alpha^3+3\,\alpha+2\,\beta^3+3\,\beta\right)\cosh\Delta-6\,\alpha \tag{34}$$

and

$$\Delta = \beta-\alpha$$

Note that the expression for B in Eq. (33) is another form of B in Eq. (21) in Masliya et al.'s paper [27].

$$H = \frac{1}{J_M}\left[-3\,\left(\alpha^3+2\,\beta^3\right)\cosh\alpha +9\,\alpha\,\left(-\beta\sinh\beta+\cosh\beta +\alpha\,\sinh\alpha-\cosh\alpha\right)\right] \tag{35}$$

$$G = \frac{(\sinh\alpha-\alpha\,\cosh\beta)\,H-3\,\alpha}{\alpha\sinh\beta-\cosh\alpha} \tag{36}$$

$$F = \frac{G\cosh\alpha+H\sinh\alpha}{3\alpha} \tag{37}$$

$$E = 2\,B+2\,F\beta^3 \tag{38}$$

$$= 1 \tag{39}$$

$$D = 0 \tag{40}$$

$$A = -B\beta^2+E+F\beta^3+(\cosh\beta-\beta\sinh\beta)\,G +(\sinh\beta-\beta\cosh\beta)\,H-\beta^3 \tag{41}$$

Masliya et al. calculated the dimensionless drag force defined as

$$\Omega_M = \frac{2B}{3\beta} \tag{42}$$

and the expression of Ω_M is

$$\Omega_M = \frac{1}{3J_M}\left[\left(-3\,\alpha^3+9\,\beta\,\alpha^2-9\,\alpha-6\,\beta^3\right)\sinh\Delta +\left(3\,\beta\,\alpha^3-9\,\alpha^2+9\,\beta\,\alpha+6\,\beta^4\right)\cosh\Delta\right] \tag{43}$$

If $a=b=R$ and $R\to\infty$, then $\Delta=0$ and $\alpha=\beta=R/\sqrt{\kappa}\to\infty$, and then $\Omega_M\to\Omega_H$.

3 Drag force exerted on cells with uniformly porous layer

In 1958 [16], Happel put Stokes' sphere into a spherical cell to develop an cell model to study fluid flow passing through a swarm of equal-sized particles swarm. In 1973 [30], Neale et al. followed Happle's approach to research fluid flow passing through a swarm of permeable spheres by adding Brinkman's model in a cell. In 2005 [21], Kim and Yuan included Masliyah's sphere in a cell to study the creeping flow over a swarm of the equal-sized composite spheres and provided the most general solution that included the five previous studies.

3.1 Happel's cell model

Happel [15] studied the motion of particles relative to a fluid flow to predict the effect of concentration of particles on their rate of steady sedimentation under the influence of gravity. The model assumed that particles are spherical, mono-dispersed and smooth. The Navier-Stokes equations without inertia terms were used to describe the fluid motion. A random assemblage consist of a number of cells, each of which contains a spherical particle surrounded by a fluid envelope; each envelope contains the same amount of fluid as the relative volume of fluid to the particle volume in the assemblage. Happel developed a sphere-in-cell model to describe the motion of fluids relative to beds of spherical particles.

Happel's cell model considered two concentric spheres: the inner sphere of a radius a representing a spherical particle, and the outer sphere of radius b the cell containing fluid and the particle at the center. It is assume that the fluid approaching in the $+Z$ direction at velocity V is steady and axi-symmetric, and this two concentric spheres are stationary having their center at the origin of spherical coordinates (r,θ,ϕ), as illustrated in Figure 4 The motion of fluid is governed by Stokes' equation with continuity equation as follows:

$$\mu\nabla^2\mathbf{u} = \nabla p, \quad a<r<b \tag{44a}$$

$$\nabla\cdot\mathbf{u} = 0, \quad a<r<b \tag{44b}$$

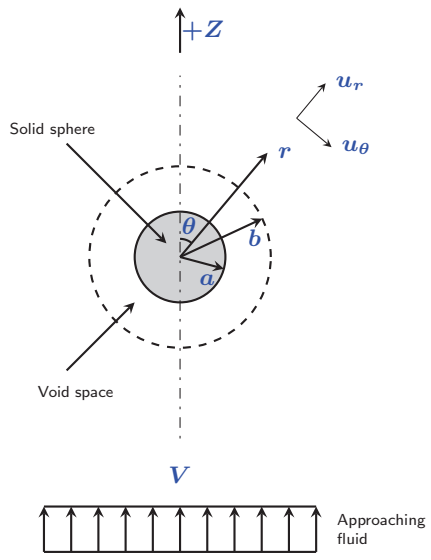

Figure 4: Coordinate system for axi-symmetric fluid flow relative to two concentric spheres comprising a solid impermeable sphere surrounded by shell of fluid

where the axi-symmetry of the fluid gives a 2-D problem. To solve the partial differential equations (44), it is assumed that the internal sphere moves with a free surface. The boundary condition is described as follows:

$$\begin{aligned} u_r(a,\theta) &= 0 && (45a)\\ u_\theta(a,\theta) &= 0 && (45b)\\ u_r(b,\theta) &= V\cos\theta && (45c)\\ \tau_{r\theta}(b,\theta) &= 0 && (45d) \end{aligned}$$

the limit of $b \to \infty$, Eqs. (45) are identical to Eqs. (3) with $a = R$.

Introducing a stream function $\psi(r,\theta)$ defined by Eq. (4), the governing equation Eq. (44) becomes an ordinary differential equation as follows:

$$E^4\psi = 0, \quad a < r < b \tag{46}$$

where E^2 is the differential operator defined by Eq. (6). Using the boundary conditions Eq. (45), the solution for Eq. (46) is calculated as

$$\psi = -\frac{Vb^2}{2}\left(\frac{A}{r} + Br + Cr^2 + Dr^4\right)\sin^2\theta, \quad a < r < b \tag{47}$$

where

$$A = \frac{b^3\eta^3}{-2-3\,\eta^5+3\,\eta+2\,\eta^6} \tag{48}$$

$$B = -\frac{b\left(3+2\,\eta^5\right)\eta}{-2-3\,\eta^5+3\,\eta+2\,\eta^6} \tag{49}$$

$$C = \frac{3\,\eta^5+2}{-2-3\,\eta^5+3\,\eta+2\,\eta^6} \tag{50}$$

and

$$D = -\frac{\eta^3}{b^2\left(-2-3\,\eta^5+3\,\eta+2\,\eta^6\right)} \tag{51}$$

where $\eta = a/b$. The solutions to components of the velocity $\mathbf{u} = (u_r, u_\theta)$ are

$$u_r = \left(-\frac{A}{r^3} - \frac{B}{r} - C - r^2D\right)\cos\theta V \tag{52}$$

and

$$u_\theta = \left(-\frac{1}{2}\frac{A}{r^3} + \frac{1}{2}\frac{B}{r} + C + 2\,r^2D\right)\sin\theta V \tag{53}$$

The dimensionless drag force Ω_H is given as

$$\Omega_H = -\frac{2}{3}\frac{2\,\eta^5+3}{2\,\eta^6-2+3\,\eta-3\,\eta^5} \tag{54}$$

The volume fraction of spherical particles in the assemblage can be described as $\phi = (a/b)^3 = \eta^3$. The Ω_H is represented as a function of ϕ as

$$\Omega_H = -\frac{2}{3}\frac{2\,\phi^{5/3}+3}{2\,\phi^2-2+3\,\phi^{1/3}-3\,\phi^{5/3}} \tag{55}$$

3.2 Neale et al.'s cell model

Neale et al. [30] discussed what Sutherland and Tan (1970) investigated analytically regarding the sedimentation characteristics of an isolated permeable sphere and came to the principal conclusion that internal permeation could be neglected, even at overall porosities in excess of 0.9. Neale et al. compared several possible solutions for the problem of creeping flow relative to an isolated permeable sphere, and found that the most satisfactory solution was based upon Brinkman's extension of Darcy's Law. This solution was generalized, using Happel's model, to cover the problem of flow relative to a swarm of permeable spheres.

For mathematical simplicity, they introduced a simple model that includes a permeable sphere of radius a composed of homogeneous and isotropic porous material of permeability κ. The fluid flow was assumed to be steady and axi-symmetric. The spherical particle was assumed to be stationary having its center at the origin of spherical coordinates (r,θ,ϕ), while the flow approaches in the $+Z$ direction with velocity V, as depicted in Fig. 5 The fluids outside

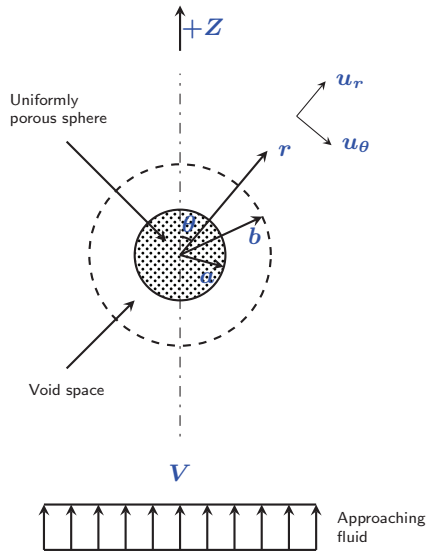

Figure 5: Coordinate system for axi-symmetric fluid flow relative to an isolated permeable sphere

and inside the permeable sphere were governed by Navier-Stokes equation and Brinkman's extension of the Darcy equation as follows,

$$\mu\nabla^2\mathbf{u} = \nabla p, \quad a < r < b \tag{56a}$$
$$\mu^*\nabla^2\mathbf{u}^* - \frac{\mu^*}{\kappa}\mathbf{u}^* = \nabla p^*, \quad 0 < r < a \tag{56b}$$

respectively, with continuity equations in corresponding regions

$$\nabla\cdot\mathbf{u} = 0, \quad a < r < b \tag{57a}$$
$$\nabla\cdot\mathbf{u}^* = 0, \quad 0 < r < a \tag{57b}$$

where $\mathbf{u} = (u_r, u_\theta, u_\phi)$, $\mathbf{u}^* = \left(u_r^*, u_\theta^*, u_\phi^*\right)$; and μ, μ^*, p, p^*, and κ^* were defined as noted earlier with the assumption of the axi-symmetric nature of the permeable sphere, the azimuthal coordinate ϕ may henceforth be suppressed. The boundary conditions were expressed as follows:

$$\lim_{r\to 0} u_r^* \text{ is finite} \tag{58a}$$
$$\lim_{r\to 0} u_\theta^* \text{ is finite} \tag{58b}$$
$$u_r(a,\theta) = u_r^*(a,\theta) \tag{58c}$$
$$u_\theta(a,\theta) = u_\theta^*(a,\theta) \tag{58d}$$
$$\tau_{rr}(a,\theta) = \tau_{rr}^*(a,\theta) \tag{58e}$$
$$\tau_{r\theta}(a,\theta) = \tau_{r\theta}^*(a,\theta) \tag{58f}$$
$$u_r(b,\theta) = V\cos\theta \tag{58g}$$
$$\tau_{r\theta}(b,\theta) = 0 \tag{58h}$$

where τ_{rr}, $\tau_{r\theta}$, τ_{rr}^* and $\tau_{r\theta}^*$ were defined by Eq. (10) and Eq. (19).

To solve the governing Eqs. (56)-(57) with boundary conditions of Eq. (58), we introduce stream functions ψ and ψ^* into Eq. (4) and Eq. (21), respectively, which should satisfy the following ordinary differential equations:

$$E^4\psi = 0, \quad a < r < b \tag{59a}$$
$$E^4\psi^* - \frac{1}{\kappa}E^2\psi^* = 0, \quad 0 < r < a \tag{59b}$$

where E^2 is defined in Eq. (6). By using the boundary conditions of Eq. (58), the general solutions for ψ and ψ^* are expressed as follows:

$$\psi = \frac{\kappa V}{2}\left(\frac{A}{\xi} + B\xi + C\xi^2 + D\xi^4\right)\sin^2(\theta), \quad \beta < \xi < \beta/\eta \tag{60a}$$
$$\psi^* = \frac{\kappa V}{2}\left[\frac{E}{\xi} + F\xi^2 + G\left(\frac{\cosh\xi}{\xi} - \sin\xi\right) + H\left(\frac{\sinh\xi}{\xi} - \cosh\xi\right)\right]\sin^2(\theta), \quad 0 < \xi < \beta \tag{60b}$$

where $\xi = r/\sqrt{\kappa}$, $\beta = a/\sqrt{\kappa}$ and $\eta = a/b$. Coefficients A, B, C, D, E, F, G and H in Eq. (60) are determined by using boundary conditions from Eq. (58) as follows:

$$A = -\frac{1}{J_{NEN}}\left[\beta^5 + 6\,\beta^3 - \frac{\tanh\beta}{\beta}\left(3\,\beta^5 + 6\,\beta^3\right)\right] \tag{61}$$

$$B = \frac{1}{J_{NEN}}\left[3\,\beta^3 + 2\,\beta^3\eta^5 + 30\,\beta\eta^5 - \frac{\tanh\beta}{\beta}\left(3\,\beta^3 + 12\,\beta^3\eta^5 + 30\,\beta\eta^5\right)\right] \tag{62}$$

$$C = -\frac{\eta\,B}{\beta} - 1 \tag{63}$$

$$D = -\frac{\eta^5 A}{\beta^5} \tag{64}$$

$$E = 0 \tag{65}$$

$$F = -\frac{B}{\beta^3} - 10\,D \tag{66}$$

$$G = 0 \tag{67}$$

$$H = \frac{1}{J_{NEN}}\left[6\,\beta^2\,(\operatorname{sech}\beta)\left(1 - \eta^5\right)\right] \tag{68}$$

where

$$J_{NEN} = 2\beta^2 - 3\beta^2\eta + 3\beta^2\eta^5 - 2\beta^2\eta^6 + 90\beta^{-2}\eta^5 + 42\eta^5 - 30\eta^6 + 3 - \frac{\tanh\beta}{\beta}\left(-3\beta^2\eta + 15\beta^2\eta^5 - 12\beta^2\eta^6 + 90\beta^{-2}\eta^5 + 72\eta^5 - 30\eta^6 + 3\right) \quad (69)$$

Similarly, the dimensionless drag force is calculated as follows:

$$\Omega_{NEN} = \frac{2B}{3\beta} \quad (70)$$

where the subscript NEN of Ω_{NEN} represents the initials of the last names of Neale, Epster and Nader [30].

3.3 Kim and Yuan's cell model

Kim and Yuan (2005b) developed a model to evaluate hydrodynamic cake resistance due to filtered aggregates. An aggregate is modeled as a hydrodynamically and geometrically equivalent solid core with a porous shell. Creeping flow past a swarm of the composite spheres was solved using Stokes' equation and Brinkman's extension of Darcy's law. They analytically calculated the dimensionless drag force Ω_{KY} exerted on the composite sphere. In certain limiting cases, Ω_{KY} converged to pre-existing analytical solutions for (i) an isolated impermeable sphere (Stokes' Model [40], (ii) an isolated uniformly porous sphere (Brinkman's Model [7]), (iii) an isolated composite sphere (Masliya et al.'s Model [27]), (iv) a swarm of impermeable spheres (Happel's Model [16]), and (v) a swarm of uniformly porous spheres (Neale et al.'s Model [30]).

From a hydrodynamic point of view, the flow through a uniform porous sphere can be categorized into two representative types: a slow interior flow driven by fluid pressure and a fast exterior flow due to shear stress around the permeable sphere surface [43]. This phenomenon is more apparent in a fractal aggregate whose central region is typically much denser than its edge. Therefore, in their work, a fractal aggregate characterized by its radius and fractal dimension is simplified to an impermeable inner core and an uniformly permeable outer shell. Following Neale et al.'s (1973a) approach, they positioned the simplified aggregate at the center of the tangential stress-free cell [30], applied proper boundary conditions, and calculated the hydrodynamic drag force exerted on a swarm of the model aggregates.

A primary assumption used in this study is that a solid spherical core surrounded by a uniformly porous shell is hydrodynamically equivalent to a fractal aggregate with radially varying permeability. For mathematical convenience, the composite sphere is assumed to be stationary having its center at the origin of spherical coordinates (r, θ, ϕ), while the flow approaches in the $-Z$ direction with a constant velocity V. The radius of the impermeable core is a; the outer radius of the porous shell with permeability κ is b $(b > a)$; and the radius of the hypothetical spherical cell of the free tangential stress is c $(c > b)$. The creeping flow of Newtonian fluid with absolute viscosity μ is considered to be steady and axi-symmetric, as shown in Fig. 6.

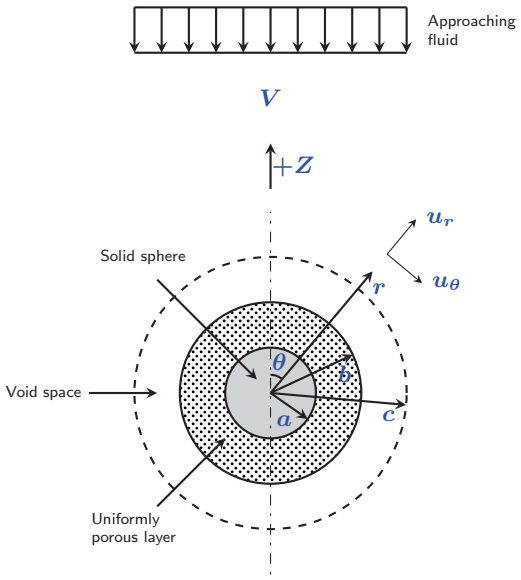

Figure 6: Coordinate system for axi-symmetric fluid flow relative to a composite sphere consisting of an impermeable solid sphere and a porous shell with tangential stress-free surface

The governing equations of incompressible Newtonian creeping flow in the void space and the porous shell covering the solid core are Stokes' equation and Brinkman's extension of Darcy's law, respectively,

$$\mu\nabla^2\mathbf{u} = \nabla p, \quad b < r < c \quad (71a)$$

$$\mu^*\nabla^2\mathbf{u}^* - \frac{\mu^*}{\kappa}\mathbf{u}^* = \nabla p^*, \quad a < r < b \quad (71b)$$

with continuity equations of

$$\nabla\cdot\mathbf{u} = 0, \quad b < r < c \quad (72a)$$

$$\nabla\cdot\mathbf{u}^* = 0, \quad a < r < b \quad (72b)$$

From the assumption of the axi-symmetric nature of the permeable sphere problem, the azimuthal coordinate ϕ was not considered. As we mentioned above,

it has been proven that the continuity of the normal stress is equivalent to that of the fluid pressure [14, 24], i.e.

$$p\left(b,\theta\right)=p^{*}\left(b,\theta\right)$$

The boundary conditions are set as follows:

$$\begin{aligned}
u_{r}^{*}\left(a,\theta\right) &= 0 && \text{(73a)}\\
u_{\theta}^{*}\left(a,\theta\right) &= 0 && \text{(73b)}\\
u_{r}^{*}\left(b,\theta\right) &= u_{r}\left(b,\theta\right) && \text{(73c)}\\
u_{\theta}^{*}\left(b,\theta\right) &= u_{\theta}\left(b,\theta\right) && \text{(73d)}\\
\tau_{rr}^{*}\left(b,\theta\right) &= \tau_{rr}\left(b,\theta\right) && \text{(73e)}\\
\tau_{r\theta}^{*}\left(b,\theta\right) &= \tau_{r\theta}\left(b,\theta\right) && \text{(73f)}\\
u_{r}\left(c,\theta\right) &= V\cos\theta && \text{(73g)}\\
\tau_{r\theta}\left(c,\theta\right) &= 0 && \text{(73h)}
\end{aligned}$$

where τ_{rr}, $\tau_{r\theta}$, τ_{rr}^{*} and $\tau_{r\theta}^{*}$ were defined by Eq. (10) and Eq. (19). To solve the governing equations (71) with the boundary conditions (73), stream functions $\psi(r,\theta)$ and $\psi^{*}(r,\theta)$ defined by Eqs. (4) and (21) are used. Then the problem is to solve the following ordinary differential equations:

$$\begin{aligned}
E^{4}\psi &= 0, \quad b<r<c && \text{(74a)}\\
E^{4}\psi^{*}-\frac{1}{\kappa}E^{2}\psi^{*} &= 0, \quad a<r<b && \text{(74b)}
\end{aligned}$$

where E^{2} is a partial differential operator defined by Eq. (6). The functional form of ψ and ψ^{*} are expressed as follows with valid radial regions:

$$\begin{aligned}
\psi &= \frac{\kappa V}{2}\left(\frac{A}{\xi}+B\xi+C\xi^{2}+D\xi^{4}\right)\sin^{2}(\theta),\\
&\qquad \beta<\xi<\gamma && \text{(75a)}\\
\psi^{*} &= \frac{\kappa V}{2}\left[\frac{E}{\xi}+F\xi^{2}+G\left(\frac{\cosh\xi}{\xi}-\sin\xi\right)\right.\\
&\quad \left.+H\left(\frac{\sinh\xi}{\xi}-\cosh\xi\right)\right]\sin^{2}(\theta),\\
&\qquad \alpha<\xi<\beta && \text{(75b)}
\end{aligned}$$

where $\xi=r/\sqrt{\kappa}$, $\alpha=a/\sqrt{\kappa}$, $\beta=b/\sqrt{\kappa}$ and $\gamma=c/\sqrt{\kappa}$. Using the boundary conditions of Eqs. (73), the coefficients $A-H$ are analytically solved, as given in Appendix A.

Using the definition of the dimensionless drag force Ω_{KY}:

$$\Omega_{KY}(\alpha,\beta,\gamma)=\frac{2B}{3\beta} \qquad (76)$$

they calculate some limiting cases of Ω_{KY}:

(i) If $\alpha\to\beta$ (or $\kappa\to 0$) and $c\to\infty$, then Stokes's equation is obtained, i.e.

$$\lim_{\gamma\to\infty}\lim_{\alpha\to\beta}\Omega_{KY}(\alpha,\beta,\gamma)=\Omega_{S}=1 \qquad (77)$$

(ii) If $\alpha\to 0$ and $\gamma\to\infty$, then Brinkman's equation [7] is replicated, i.e.,

$$\lim_{\gamma\to\infty}\lim_{\alpha\to 0}\Omega_{KY}(\alpha,\beta,\gamma)=\Omega_{B} \qquad (78)$$

(iii) If $\gamma\to\infty$, then Masliya's expression [27] is reproduced, i.e.,

$$\lim_{\gamma\to\infty}\Omega_{KY}(\alpha,\beta,\gamma)=\Omega_{M} \qquad (79)$$

(iv) If $\alpha\to\beta$ (or $\kappa\to 0$) and $\eta=c/b$, then Happel's formula [16] is retrieved, i.e.,

$$\lim_{\alpha\to\beta}\Omega_{KY}(\alpha,\beta,\gamma)=\Omega_{H} \qquad (80)$$

(v) If $\alpha\to 0$, then Neale et al.'s work [30] is obtained, i.e.,

$$\lim_{\alpha\to 0}\Omega_{KY}(\alpha,\beta,\gamma)=\Omega_{NEN} \qquad (81)$$

The above comparison is summarized in the following figure.

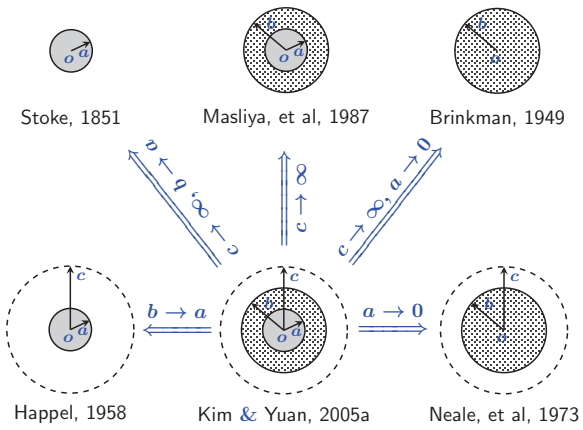

Figure 7: Comparisons between Kim & Yuan's cell model with a porous layer with the uniformly permeability and other previous works

Appendix: Expressions of the coefficients from A to H of stream functions in Kim and Yuan's cell model

$$\begin{aligned}
A= &-B\beta^{2}-C\beta^{3}-D\beta^{5}+E+F\beta^{3}\\
&+\left(\cosh\beta-\beta\sinh\beta\right)G\\
&+\left(\sinh\beta-\beta\cosh\beta\right)H
\end{aligned} \qquad (82)$$

$$
\begin{aligned}
B = \; & \frac{1}{J_{KY}} \left\{ \left[\left(-\frac{9}{2}\,\alpha\,\beta - \frac{3}{2}\,\beta\,\alpha^3 \right.\right.\right. \\
& -3\,\beta^4 + \frac{9}{2}\,\alpha^2 \Big) \cosh\Delta \\
& + \left(\frac{3}{2}\,\alpha^3 - \frac{9}{2}\,\beta\,\alpha^2 \right. \\
& \left.\left. + \frac{9}{2}\,\alpha + 3\,\beta^3 \right) \sinh\Delta \right] C \\
& + \left[15\,\beta^3\alpha + \left(-\frac{15}{2}\,\beta^3\alpha \right.\right. \\
& -30\,\beta^4 + \frac{45}{2}\,\beta^2\alpha^2 \\
& \left. -5\,\beta^6 - \frac{15}{2}\,\beta^3\alpha^3 \right) \cosh\Delta \\
& + \left(30\,\beta^3 - \frac{15}{2}\,\beta^3\alpha^2 + \frac{45}{2}\,\beta^2\alpha \right. \\
& \left.\left. \left. + \frac{15}{2}\,\alpha^3\beta^2 + 15\,\beta^5 \right) \sinh\Delta \right] D \right\}
\end{aligned} \tag{83}
$$

where

$$
\begin{aligned}
J_{KY} = \; & -6\,\alpha + \left(-3 + 3\,\alpha^2\right) \sinh\Delta \\
& \left(3\,\alpha + 3\,\beta + 2\,\beta^3 + \alpha^3\right) \cosh\Delta
\end{aligned} \tag{84}
$$

$$
\begin{aligned}
C = \; & \frac{1}{C_0} \left\{ \left[\left(-\frac{1}{3} \left(12 - 12\,\alpha^2\right) \sinh\Delta \right.\right.\right. \\
& -\frac{1}{3} \left(-4\,\alpha^3 - 8\,\beta^3 - 12\,\beta \right. \\
& \left.\left. -12\,\alpha) \cosh\Delta - 8\,\alpha \right) \gamma^5 \\
& + \left(-\frac{1}{3} \left(15\,\beta^3\alpha^2 - 60\,\beta^3 - 30\,\beta^5 \right.\right. \\
& \left. -15\,\alpha^3\beta^2 - 45\,\beta^2\alpha\right) \sinh\Delta \\
& -\frac{1}{3} \left(60\,\beta^4 - 45\,\beta^2\alpha^2 + 15\,\beta^3\alpha \right. \\
& \left. +5\,\beta^3\alpha^3 + 10\,\beta^6\right) \cosh\Delta \\
& \left. + 10\,\beta^3\alpha \right) \gamma^2 \\
& -\frac{1}{3} \left(288\,\beta^5 + 360\,\beta^3 + 90\,\beta^4\alpha \right. \\
& +60\,\beta^7 + 30\,\beta^4\alpha^3 \\
& \left. -360\,\beta^3\alpha^2 - 18\,\alpha^2\beta^5\right) \sinh\Delta \\
& -\frac{1}{3} \left(-360\,\beta^3\alpha - 168\,\beta^6 - 6\,\alpha^3\beta^5 \right. \\
& +90\,\alpha^2\beta^4 - 360\,\beta^4 - 12\,\beta^8 \\
& -18\,\alpha\,\beta^5 - 120\,\beta^3\alpha^3) \cosh\Delta \\
& \left. - 240\,\beta^3\alpha - 72\,\alpha\,\beta^5 \right] D \\
& + \left[-4\,\alpha + \left(-2 + 2\,\alpha^2\right) \sinh\Delta \right. \\
& + \left(2\,\alpha + \frac{4}{3}\,\beta^3 + \frac{2}{3}\,\alpha^3 + 2\,\beta \right) \cdot \\
& \left. \left. \cdot \cosh\Delta \right] \gamma^3 \right\}
\end{aligned} \tag{85}
$$

where

$$
\begin{aligned}
C_0 = \; & \left[\left(2 - 2\,\alpha^2\right) \sinh\left(\Delta\right) \right. \\
& + \left(-\frac{2}{3}\,\alpha^3 - 2\,\alpha - 2\,\beta \right. \\
& \left. \left. -\frac{4}{3}\,\beta^3 \right) \cosh\Delta + 4\,\alpha \right] \gamma^3 \\
& + \left[\left(-2\,\beta^3 - \alpha^3 - 3\,\alpha \right.\right. \\
& \left. + 3\,\beta\,\alpha^2\right) \sinh\Delta \\
& + \left(2\,\beta^4 - 3\,\alpha^2 + \beta\,\alpha^3 \right. \\
& \left. \left. +3\,\alpha\,\beta\right) \cosh\Delta \right] \gamma^2 \\
& + \left(4\,\beta^5 + 8\,\beta^3 + 2\,\alpha^3\beta^2 \right. \\
& +6\,\beta^2\alpha - 2\,\beta^3\alpha^2\big) \sinh\Delta \\
& + \left(-2\,\beta^3\alpha - \frac{4}{3}\,\beta^6 + 6\,\beta^2\alpha^2 \right. \\
& \left. -8\,\beta^4 - \frac{2}{3}\,\beta^3\alpha^3 \right) \cosh\Delta + 4\,\beta^3\alpha
\end{aligned} \tag{86}
$$

$$
\begin{aligned}
D = \; & \frac{1}{D_0} \left[\left(-12\,\beta^3 - 6\,\beta^5 + 3\,\beta^3\alpha^2 \right.\right. \\
& -9\,\beta^2\alpha - 3\,\alpha^3\beta^2\big) \sinh\Delta \\
& + \left(2\,\beta^6 + 12\,\beta^4 - 9\,\beta^2\alpha^2 + \beta^3\alpha^3 \right. \\
& \left. \left. +3\,\beta^3\alpha\right) \cosh\Delta - 6\,\beta^3\alpha \right] \gamma
\end{aligned} \tag{87}
$$

where

$$
\begin{aligned}
D_0 = \; & \left[\left(-6 + 6\,\alpha^2\right) \sinh\Delta - 12\,\alpha \right. \\
& \left. + \left(2\,\alpha^3 + 6\,\beta + 4\,\beta^3 + 6\,\alpha\right) \cosh\Delta \right] \gamma^6 \\
& + \left[\left(9\,\alpha - 9\,\beta\,\alpha^2 + 3\,\alpha^3 + 6\,\beta^3\right) \sinh\Delta \right. \\
& \left. + \left(9\alpha^2 - 6\beta^4 - 3\beta\alpha^3 - 9\alpha\beta\right) \cosh\Delta \right] \gamma^5 \\
& + \left[-108\,\alpha\,\beta^5 - 360\,\beta^3\alpha - 30\,\beta^7 \right. \\
& + \left(-15\,\beta^4\alpha^3 - 144\,\beta^5 \right. \\
& -180\,\beta^3 + 180\,\beta^3\alpha^2 \\
& \left. +9\,\alpha^2\beta^5 - 45\,\beta^4\alpha\right) \sinh\Delta \\
& + \left(-45\,\alpha^2\beta^4 + 180\,\beta^4 + 180\,\beta^3\alpha \right. \\
& +84\,\beta^6 + 3\,\alpha^3\beta^5 + 9\,\alpha\,\beta^5 \\
& \left. \left. +60\,\beta^3\alpha^3 + 6\,\beta^8\right) \cosh\Delta \right] \gamma \\
& + \left(24\,\beta^8 + 270\,\beta^3\alpha + 60\,\beta^6 \right. \\
& -6\,\beta^6\alpha^2 + 90\,\beta^3\alpha^3 - 270\,\alpha^2\beta^4 \\
& +36\,\alpha\,\beta^5 + 12\,\alpha^3\beta^5\big) \sinh\Delta \\
& + \left(-4\,\beta^9 - 60\,\beta^7 + 36\,\alpha^2\beta^5 \right. \\
& -6\,\alpha\,\beta^6 - 90\,\beta^4\alpha^3 - 270\,\beta^4\alpha - 2\,\beta^6\alpha^3 \\
& \left. +270\,\beta^3\alpha^2\right) \cosh\Delta + 120\,\alpha\,\beta^6
\end{aligned} \tag{88}
$$

$$
E = 20\,D\beta^3 + 2\,B + 2\,F\beta^3 \tag{89}
$$

$$
F = \frac{1}{3}\,\frac{G\cosh\alpha + H\sinh\alpha}{\alpha} \tag{90}
$$

$$
\begin{aligned}
G = \; & -\frac{\left(\alpha\cosh\beta - \sinh\alpha\right) H}{\alpha\sinh\beta - \cosh\alpha} \\
& -\frac{15\,\alpha\beta^2 D + 3\,\alpha\,C}{\alpha\sinh\beta - \cosh\alpha}
\end{aligned} \tag{91}
$$

and

$$H = \frac{1}{J_{KM}} \{ [9\,\alpha^2 \sinh\alpha - 9\,\beta\,\alpha \sinh\beta + \left(-9\,\alpha - 6\,\beta^3 - 3\,\alpha^3\right)\cosh\alpha + 9\,\alpha\cosh\beta]\,C + [45\,\alpha^2\beta^2 \sinh\alpha + 45\,\alpha\beta^3 \sinh\beta + 45\,\beta^2\alpha\cosh\beta + \left(-45\,\beta^2\alpha - 30\,\beta^5 - 15\,\alpha^3\beta^2 - 90\,\beta^3\right)\cosh\alpha]\,D \} \quad (92)$$

Acknowledgements: The research was supported by the US National Science Foundation (CBET-0444931(CAREER) and CBET-0552413), and Qingdao Univeristy (grant No.06300371). The author would like to thank Prof. Albert S. Kim for his support and help when the author was studying at University of Hawaii at Manoa.

References

[1] R. Amal, J.- A. Rapper, and T.-D. Waite, Fractal structure of hematite aggregates, *J. Colloid Interface Sci.* 140, 1990, pp. 158-168.

[2] A. Bagga, S. Chellam, and D.- A. Clifford, Evaluation of iron chemical coagulation and electro-coagulation pretreatment for surface water microfiltration, *J. Membrane Sci.* 309, 2008, pp. 82-93.

[3] G. Belfort, R.-H. Davis, and A.-L. Zydney, The behavior of suspensions and macromolecular solutions in crossflow microfiltration, *J. Membrane Sci.* 96, 1994, pp. 1-58.

[4] S. Bhattacharjee, A.-S. Kim, and M. Elimelech, Concentration polarization of interacting solute particles in cross-flow membrane filtration, *J. Colloid Interface Sci.* 212, 1999, pp. 81-99.

[5] S. Bhattacharjee, A. Sharma, and P.-K. Bhattacharya, A unified model for flux prediction during batch cell ultrafiltration, *J. Membrane Sci.* 111, 1996, pp. 243-258.

[6] B. Blankert, B.-H.-L. Betlem, and B. Roffel, Development of a control system for in-line coagulation in an ultrafiltration process, *J. Membrane Sci.* 301, 2007, pp. 39-45.

[7] H.-C. Brinkman, On the permeability of media consisting of closely packed porous particles, *Appl. Sci. Res.* 1, 1949, pp. 81-86.

[8] T. Carroll, S. King, S.-R. Gray, B.-A. Bolto, and N.-A. Booke, The fouling of microfiltration membranes by nom after coagulation treatment, *Wat. Res.* 34, 2000, pp. 2861-2868.

[9] M.-W. Chudacek and A.-G. Fane, The dynamics of polarisation in unstirred and stirred ultrafiltration, *J. Membrane Sci.* 21, 1984, pp. 145-160.

[10] K.-J. Dunn and D. J Bergman, Self diffusion of nuclear spins in a porous medium with a periodic microstructure, *J. Chem. Phys.* 102, 1995, pp. 3041-3054.

[11] M. Elimelech and S. Bhattacharjee, A novel approach for modeling concentration polarization in crossflow membrane filtration based on the equivalence of osmotic pressure model and filtration theory,*J. Membrane Sci.* 145, 1998, pp. 223-241.

[12] R.-S. Faibish, M. Elimelech, and Y. Cohen, Effect of interparticle electrostatic double layer interactions on permeate flux decline in crossflow membrane filtration of colloidal suspensions: An experimental investigation, *J. Colloid Interface Sci.* 204, 1998, pp. 77-86.

[13] R.-J. Francois and A.-A. Van Haute, Structure of hydroxide flocs, *Wat. Res.* 19, 1985, pp. 1249-1254.

[14] S. Haber and R. Mauri, Boundary conditions for darcy's flow through porous media, *Int. J. Multiphase Flow* 9, 1983, pp. 561-574.

[15] J. Happel, Viscosity of suspensions of uniform spheres, *J. Appl. Phys.* 28, 1957, pp. 1288-1292.

[16] J. Happel, Viscous flow in multiparticle systems: slow motion of fluids relative to beds of spherical particles, *AIChE J.* 4, 1958, pp. 197-201.

[17] U. Hizi and D.-J. Bergman, Molecular diffusion in periodic porous media, *J. Appl. Phys.* 87, 2000, pp. 1704.

[18] E.-M.-V. Hoek, A.-S. Kim, and M. Elimelech, Influence of crossflow membrane filter geometry and shear rate on colloidal fouling in reverse osmosis and nanofiltration separations, *Environ. Eng. Sci.* 19, 2002, pp. 357-372.

[19] A.-S. Kim and E.-M.-V. Hoek, Cake structure in dead-end membrane filtration: Monte carlo simulations, *Environ. Eng. Sci.* 19,2002, pp. 373-386.

[20] A.-S. Kim and K.-D. Stolzenbach, The permeability of synthetic fractal aggregates with realistic three-dimensional structure, *J. Colloid Interface Sci.* 253, 2002, pp. 315-328.

[21] A.-S. Kim and R. Yuan, A new model for calculating specific resistance of aggregated colloidal cake layers in membrane filtration processes, *J. Membrane Sci.* 249, 2005, pp. 89-101.

[22] R.-C. Klimpel and R. Hogg, Effects of flocculation conditions on agglomerate structure, *J. Colloid Interface Sci.* 113, 1986, pp. 121-131.

[23] J. Koplik, L. Herbert, and A. Zee, Viscosity renormalization in brinkman equation, *Phys. Fluids* 26, 1983, pp. 2864-2870.

[24] S.-A. Lee, A.-G. Fane, R. Amal, and T.-D. Waite, The effect of floc size and structure on specific cake resistance and compressibility in dead-end microfiltration, *Sep. Sci. Tech.* 38, 2003, pp. 869-887.

[25] D.-H. Li and J.-J. Ganczarczyk, Stroboscopic determination of settling velocity, size and porosity of activated sludge flocs, *Wat. Res.* 21, 1987, pp. 257-262.

[26] B.-E. Logan and D.-B. Wilkinson, Fractal dimensions and porosities of zoogloea ramigera and saccharom yces cerevisae aggregates, *Biotech. Bioeng.* 38, 1991, pp. 389-396.

[27] J.-H. Masliyah, G.-H. Neale, K. Malysa, and T.-G.-M Van De Ven, Creeping flow over a composite sphere: Solid core with porous shell, *Chem. Eng. Sci.* 42, 1987, pp. 245-253.

[28] K. Matsumoto and A. Suganuma, Settling velocity of a permeable model floc, *Chem. Eng. Sci.* 32, 1977, pp. 445-447.

[29] A.-S. Michaels, New separation technique for the cpi, *Chem. Eng. Prog.* 64, 1968, pp. 31.

[30] G.-H. Neale, N. Epstein, and W. Nader, Creeping flow relative to permeable spheres, *Chem. Eng. Sci.* 28, 1973, pp. 1865-1874.

[31] G. Ooms, P.-F. Mijnlieff, and H.-L. Beckers, Frictional force exerted by a flowing fluid on a permeable particle, with particular reference to polymer coils, *J. Chem. Phys.* 53, 1970, pp. 4123.

[32] P.-K. Park, C.-H. Lee, and S. Lee, Determination of cake porosity using image analysis in a coagulation-microfiltration system, *J. Membrane Sci.* 293, 2007, pp. 66-72.

[33] C.-A. Romero and R.-H. Davis, Global model of crossflow microfiltration based on hydrodynamic particle diffusion, *J. Membrane Sci.* 39, 1988, pp. 157-185.

[34] C.-A. Romero and R.-H. Davis, Transient model of crossflow microfiltration, *Chem. Eng. Sci.* 45, 1990, pp. 13-25.

[35] C.-A. Romero and R.-H. Davis, Experimental verification of the shear-induced hydrodynamic diffusion model of crossflow microfiltration, *J. Membrane Sci.* 62, 1991, pp. 249-273.

[36] M.-M. Sharp and I.-C. Escobar, Effects of dynamic or secondary-layer coagulation on ultrafiltration, *Desalination* 188, 2006, pp. 239-249.

[37] L. Song, Flux decline in crossflow microfiltrationand ultrafiltration: mechanisms and modeling of membrane fouling, *J. Membrane Sci.* 139, 1998, pp. 183-200.

[38] L. Song, A new model for the calculation of the limiting flux in ultrafiltration, *J. Membrane Sci.* 144, 1998, pp. 173-185.

[39] L. Song and M. Elimelech, Theory of concentration polarization in crossflow filtration, *J. Chem. Soc. Faraday. Trans.* 91, 1995, pp. 3389-3398.

[40] G.-G. Stokes, On the effect of internal friction of fluids on the motion of pendulums, *Trans. Camb. Phil. Soc.* 9, 1851, pp. 1-106.

[41] S. Stoll, A. Elaissari, and E. Pefferkorn, Fractal dimensions of latex aggregates: Correlation between hydrodynamic radius and cluster size, *J. Colloid Interface Sci.* 140, 1990, pp. 98-104.

[42] K.-D. Stolzenbach, Scavenging of small particles by fast-sinking porous aggregates, *Deep Sea Res.* 40, 1993, pp. 359-369.

[43] D.-N. Sutherland and C.-T. Tan, Sedimentation of a porous sphere, *Chem. Eng. Sci.* 25, 1970, pp. 1948-1950.

[44] N. Tambo and Y. Watanabe, Physical characteristics of flocs-i. the floc density function and aluminium floc, *Wat. Res.* 13, 1979, pp. 409-419.

[45] M. Vanni, Creeping flow over spherical permeable aggregates, *Chem. Eng. Sci.* 55, 2000, pp. 685-698.

[46] S. Veerapaneni and M.-R. Wiesner, Hydrodynamics of fractal aggregates with radially varying permeability, *J. Colloid Interface Sci.* 177, 1996, pp. 45-57.

[47] J.-G. Wijmans, S. Nakao, J.-W.-A. Van Den Berg, F.-R. Troelstra, and C.-A. Smolders, Hydrodynamic resistance of concentration polarization boundary layers in ultrafiltration, *J. Membrane Sci.* 22, 1985, pp. 117-135.

[48] J.-G. Wijmans, S. Nakao, and C.-A. Smolders, Flux limitation in ultrafiltration: Osmotic pressure model and gel layer model, *J. Membrane Sci.* 20, 1984, pp. 115-124.